On the Mechanism of Cathodic Protection and Its Implications on Criteria Including AC and DC Interference Conditions

Markus Büchler[‡]

In recent years, a wide agreement with respect to the processes associated with cathodic protection (CP) has been reached within the CP industry. The increase of the pH value at the steel surface and the generation of passivating conditions as a result of the CP current are widely accepted as the relevant underlying mechanism. Based on this understanding it was possible to identify the relevant processes with respect to AC and DC interference and explain the empirical observations. This led to the development of ISO 18086 and has significantly influenced the work on ISO/DIS 21857. This paper summarizes present state of knowledge, the more recent developments, and their implications with respect to the CP criteria. It summarizes the relevant aspects in association with interference conditions and highlights possible future approaches with respect to the assessment of the effectiveness of CP.

KEY WORDS: cathodic protection, criteria, mechanism, steel

INTRODUCTION

The application of cathodic protection (CP) is generally statutory for high-pressure gas and oil pipelines. Moreover, CP is frequently used for water pipelines and buried containers. The relevant underlying principles and protection criteria are stated in ISO 15589-1. In the last years, various investigations with respect to CP have raised the understanding that the pH is an important parameter in providing the corrosion protection.[1-7] In many cases relatively small protection current densities in the range of a few tens of mA/m^2 result in an increase of the pH value at the steel surface of coating defects of pipelines. This increase of the pH favors the formation of a passive film, which significantly limits any further corrosion. By means of model calculations, which are based on thermodynamic and kinetic data, all currently used protection criteria in CP can readily be explained when taking into account the relevance of the pH and the formation of a passive film.[8] Based on these considerations, the accumulation of alkalinity and hence the mass transport at the steel surface are key determining factors in the effectiveness of CP. These aspects and the associated implications are discussed in detail by Angst, et al.[6] Today's understanding of the mechanisms involved in CP provide a new view on the protection criteria and the processes taking place during interference conditions. This far reaching understanding has led to the development of ISO 18086 for the assessment of AC corrosion and has significantly influenced the work on ISO/DIS 21857 with respect to stray current interference.

The understanding of the processes taking place during CP have led to conclusive models with respect to interference conditions. Based on these concepts it is today possible to determine the effectiveness of CP based on a new approach that is presented. The main advantage of this new concept is its applicability to all types of pipelines independent on their interference conditions as discussed by Büchler.[9-10] It is now possible to base the assessment of CP on the readily measurable on-potential and AC voltage, rather than the IR-free potential that can typically only be determined by means of coupon measurements. These new possibilities are discussed and highlighted based on an example interference situation of a pipeline.

THE MECHANISM OF CATHODIC PROTECTION

There is general agreement that the effectiveness of CP is based on polarization of the steel surface.[11-13] However, the actual chemical process that causes the polarization is often not further discussed despite its important consequences on various aspects of the effectiveness of CP. According to ISO 8044, the polarization and the associated change of potential of a steel surface is caused by the cathodic current. This polarization can be achieved through activation polarization. This cathodic shift of the potential caused by activation polarization will result in a certain decrease of the corrosion rate as described by Tafel slopes or Butler–Volmer kinetics. However, the current densities required for achieving a relevant decrease of the corrosion rate purely on activation polarization associated with a potential shift of 100 mV are higher than 0.8 A/m^2 as demonstrated with numerical models[8] and as emphasized by Angst.[7] Such current densities are usually not achieved in CP and are often associated with IR-free potentials more negative than −1.2 V_{CSE}. Such levels of polarization may cause over-polarization according to ISO 15589-1 and AC

Submitted for publication: September 5, 2019. Revised and accepted: February 17, 2020. Preprint available online: February 18, 2020, https://doi.org/10.5006/3379. First presented at the Australasian Corrosion Association's 2019 International Symposium, held July 24-25, 2019, Melbourne, Australia.
‡ Corresponding author. E-mail: markus.buechler@sgk.ch. Swiss Society for Corrosion Protection (SGK) Technoparkstrasse 1 8005 Zurich, Switzerland.

ISSN 0010-9312 (print), 1938-159X (online)

corrosion according to ISO 18086. Correspondingly, the typical current densities applied in CP in the range of 20 mA/m^2 to 1,000 mA/m^2 would not result in satisfactory activation polarization of more than 100 mV and associated corrosion protection. The cathodic current, however, inadvertently results in a change of the soil composition as a result of the electrochemical reactions taking place. The change of potential caused by this concentration change is called concentration polarization. According to von Baeckmann the activation polarization is achieved within milliseconds as a result of the current flow through the steel surface and the concentration polarization is built up within a fraction of a second, minutes, or even hours.[14] Based on the present model concepts a clearly more differentiated understanding is available today with respect to the involved electrochemical processes: it is nowadays widely accepted that the effectiveness of CP is achieved by activation polarization and the resulting concentration polarization associated with oxygen reduction and the increase of the pH value at the steel surface. The concentration polarization at the steel surface as a result of the CP current changes the composition of the soil not only in the immediate vicinity of the steel surface but also in the surrounding environment. This effect of activation and associated concentration polarization provokes a shift of both the pH and the potential along the hydrogen equilibrium line (arrows in Figure 1). The increase of the pH at the steel surface and in the surrounding soil, as well as the formation of conditions conducive to passivation, are illustrated in Figure 3(a). Because the hydrogen equilibrium potential, which correlates with the cathodic limit of water stability, depends on the pH (hydrogen evolution line in Figure 1), the pH value at the steel surface can directly be determined based on the IR-free potential. This has been discussed in detail by Angst, et al.[6] For this reason, the protection potentials according to ISO 15589-1 can readily be explained:

- The $E_{IR\text{-}free}$ of –0.85 V_{CSE} corresponds to a pH of 9 (circle on the left of Figure 1), which is sufficient for achieving passivity in normal soil conditions.
- The $E_{IR\text{-}free}$ of –0.95 V_{CSE} corresponds to a pH of 10.5 (circle in the middle of Figure 1), which allows for passivity even in aggressive soils.
- On the other hand, the $E_{IR\text{-}free}$ of –1.2 V_{CSE} corresponds to a pH of about 13 (circle to the right in Figure 1), which, according to ISO 15589-1, may cause problems with the adhesion of coatings due to over-polarization.

The position of the circles in Figure 1 is determined based on numerical modeling as discussed in Büchler.[8] Meeting these IR-free potentials will result in corrosion rates below 0.01 mm/y according to ISO 15589-1. It should be noted in this context that a pH value of 13 is typical for concrete. In concrete, the formation of a protective passive film and the resulting corrosion protection for the steel reinforcement are well accepted. Furthermore, in concrete, the conditions with respect to corrosion are considered to be critical when the pH drops below 9 as a result of carbonation. The experience associated with the corrosion protection of steel in concrete is hence associated with the same pH range from 9 to 13 as in the case of steel under CP in soils.

The dependence of the pH value at the steel surface on the CP current density has been investigated by several authors. The results are shown in Figure 2. It can be concluded that cathodic current densities in the range from 20 mA/m^2 to 1,000 mA/m^2, which are typical for the CP of the exposed steel within the coating defects on buried pipelines, result in surface pH levels from 10.5 to 12.5. According to Figure 1, these levels correlate with IR-free potentials in the range from –0.95 V_{CSE} to –1.2 V_{CSE}. Correspondingly, it is readily possible to plot the IR-free potential associated with the achieved surface pH value as shown on the right vertical axis in Figure 2. This consideration shows the relevance of the current density, the surface pH, the passivation, as well as the protection criteria based on IR-free

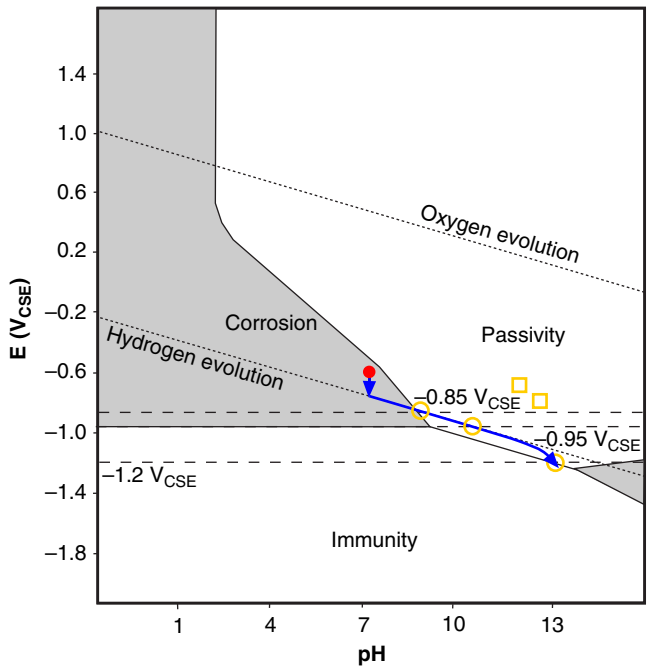

FIGURE 1. *Pourbaix-diagram (Fe/H_2O) illustrating the cathodic polarization of steel[15] as a result of activation and concentration polarization. The arrow shows the effect of polarization and the resulting increase of the pH level. The circles and squares indicate the position of the protection potentials according to ISO 15589-1.*

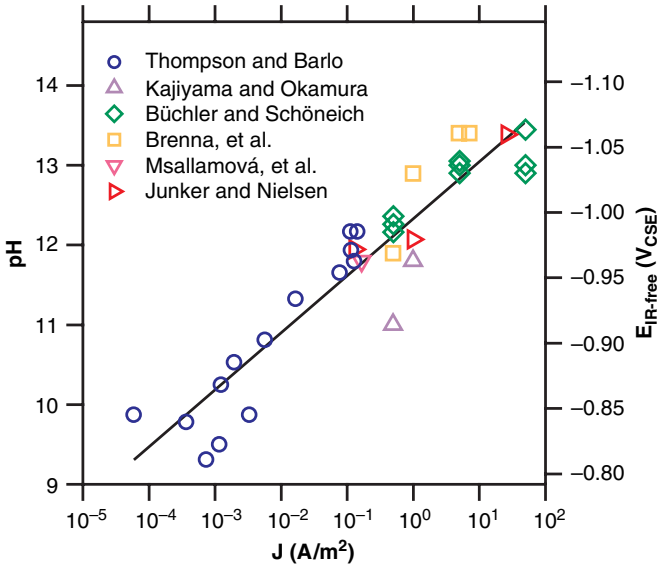

FIGURE 2. *The pH value at the steel surface as a function of the cathodic current density according to different literature sources summarized in Junker and Nielsen.[17-21] On the right vertical axis, the expected IR-free potentials associated with the hydrogen equilibrium line are shown.*

potentials for the practical implementation of CP on buried pipelines.

This discussion clearly demonstrates that the IR-free potential of the polarized steel surface is not directly linked to the corrosion protection of the steel. Instead, it corresponds to a pH measurement based on the hydrogen electrode. Because an increase in pH is associated with passivation, corrosion protection is achieved. This view was emphasized by Freiman, et al.,[1] and is today widely accepted. The textbook by Peabody[16] on CP published in 2001 made it clear that the concept of activation polarization is too simplistic to explain the time-dependent effects on cathodically protected pipelines. Instead, the pH increase at the steel surface as a result of the concentration polarization was identified to be the main factor affecting the corrosion process. This increased pH would result in the formation of a protective passive film. Hence, the concepts shown in Figure 1 are fully in line with the mechanism of CP presented in Peabody.[16]

The relevance of passivation reveals another highly relevant aspect that immediately follows from Figure 1: the IR-free potential is not suitable for assessing the corrosion situation of a passive steel surface under CP. Passivity is present at increased pH over a wide potential range extending from the hydrogen evolution line all of the way to the oxygen evolution line. In well-aerated resistive soils, it may not be possible to achieve a sufficiently high current density to polarize the steel surface to the hydrogen evolution line. The resulting IR-free potential may well be in the range of –0.65 V_{CSE} and –0.75 V_{CSE}, as shown in Figure 1 with the squares. The position of the squares in Figure 1 is determined based on numerical modeling, as discussed in Büchler.[8] As long as the pH is increased, passivity and hence corrosion protection is achieved under such conditions.[8] This immediately explains the corresponding protection criteria determined by Funk, et al.,[20] that are stated today in ISO 15589-1.

It follows that no correlation between the corrosion rate and the IR-free potential may be expected. Indeed, such a correlation has never been reported under cathodic polarization. Instead, even acceptable corrosion rates are reported at IR-free potentials as positive as 0.0 V_{CSE}.[6] This is due to the fact that the IR-free potential may only be used as a pH measurement when the IR-free potential of the steel is controlled by the hydrogen electrode. At increased aeration of the soil this is not the case and the IR-free potential becomes an irrelevant number with respect to the assessment of the achieved pH and hence the level of corrosion protection.

This consideration raises the question with respect to an alternative and more appropriate protection criterion. Based on Figure 2, a current density in the range of 1 mA/m^2 is sufficient to increase the pH to a level that allows for passivation. At such low current densities, the IR error is negligible in most soils and corrosion protection is achieved as soon as the on-potential is more negative than –0.85 V_{CSE}. This is fully in line with the concepts and protection criterion proposed by Kuhn.[11] A more recent analysis of the two most extensive field investigations with respect to CP protection criteria performed so far has clearly shown that the on-potential is at least as reliable as the IR-free potential with respect to the assessment of corrosion protection on coupons,[21] which is fully in line with the above discussion. This raises the question with respect to the appropriate level of on-potential that provides sufficient pH increase and passivation. This level predominantly depends on the bedding conditions (see Angst, et al.[6]) but also the coating defect size and the soil resistivity. The key parameter is the so-called reference current density J_{ref} that is required to increase the pH and establish effective CP. The reference on-potential that is required to ensure J_{ref} on all coating defects is called E_{ref} according to DVGW GW 21.[22] For well-bedded pipelines in sand and soil with small coating defects, E_{ref} may be as positive as –0.85 V_{CSE}. Based on Angst, et al.,[6] a value of –1.0 V_{CSE} is suggested for such conditions, because this on-potential ensures current entering into all coating defects.

THE EFFECT OF ANODIC STRAY CURRENT INTERFERENCE

There is wide agreement in literature that temporary anodic current discharge results in limited corrosion.[5,23-28] The efficiency of the anodic current with respect to anodic metal dissolution is typically very limited. These observations are difficult to explain with a concept of CP that is based on activation polarization. However, it is well in line with the concepts associated with an increase of the surface pH and the formation of a passive film. It follows from the above consideration based on concentration polarization that the CP of steel is a result of the increase of the pH value and the resulting passivity. This discussion illustrates that the assessment of stray current interference of cathodically protected pipelines needs to be reassessed in the light of today's knowledge: the limited corrosion observed during anodic current discharge can readily be explained with passivity. The present mechanistic models, the available literature, as well as empirical data allow the development of new interference assessment concepts and corresponding thresholds. These will be presented and discussed in the following.

The CP based on passivity has far reaching consequences for the assessment of time-variant stray current interference of a cathodically protected pipeline. The IR-free potential is a pH measurement rather than a controlling parameter for the assessment of the level of corrosion protection.

This has immediate consequences on the assessment of the corrosion risk under interfered conditions: the temporary anodic shift of the IR-free potential of a passive steel surface in the positive direction as a result of a temporary anodic stray current interference is not linked to a corrosion process. The IR-free potential more positive than the protection criterion of e.g., –0.95 V_{CSE} is only the result of an influenced and hence irrelevant pH measurement. In the case of well-aerated soils, IR-free potentials of –0.65 V_{CSE} and –0.75 V_{CSE} are required for addressing this influencing effect of oxygen according to ISO 15589-1. Similarly, IR-free potentials of –0.85 V_{CSE} and –0.95 V_{CSE} are no longer applicable under anodic interference, as the current turns the pH measurement based on the IR-free potential associated with the hydrogen electrode into a meaningless number. If the IR-free potential is more positive than the corresponding protection criterion during anodic stray current discharge, this does not have to be interpreted as an insufficient level of corrosion protection in the case of a temporary anodic interference.

Time-variant interference is typically caused by DC-operated railways or trams. In these cases, the anodic interference has usually a maximum duration of about 250 s. In contrast, time-variant anodic stray current discharge from coating defects on pipelines under AC interference occurs at much higher frequency resulting anodic current discharge for only about 10 ms. Moreover, telluric interference is well known to cause time-variant interference at very low frequency with anodic interference duration in the range of up to several hours. It is evident from the above discussion that a time-limited

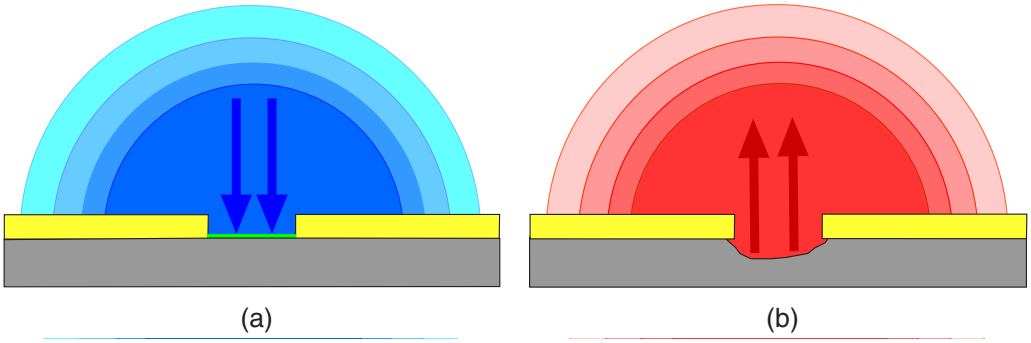

FIGURE 3. *Schematic illustration of (a) cathodic concentration polarization and (b) anodic concentration polarization. The cathodic current entering the steel surface results in a depletion of oxygen, an increase of the pH value in the soil, and passivation (a). The anodic current leaving the steel surface results in a lowering of the pH value and provokes corrosion (b). The intensity of coloring indicates the extent of pH change.*

anodic current discharge cannot result in corrosion. In fact, the anodic polarization will only shift the potential in the positive direction within the passive domain, which usually does not result in corrosion. The anodic charge will rather be consumed for the oxidation of ferrous ions (Fe(II)) within the oxide layers on the steel surface as described in Büchler and Schöneich.[3] As a consequence, the repeated cathodic and anodic interference caused by DC-operated railways or trams will result in a relevant charge transfer through the steel surface. This electric charge, however, will not be consumed by the corrosion reaction, but will be used for the redox system Fe(II)/Fe(III)/Fe(II). In Figure 4 this redox system based on magnetite/maghemite is indicated with the dashed line. Bette observed this phenomenon already in 2005[29] and described it with capacitive charging effects. In fact, the above-mentioned redox system acts as a pseudo-capacity and may readily be compared to the charging/discharging of an accumulator. Consequently, the combination of passivity with this redox system explains the empirical observation that a time-limited anodic current will neither result in major anodic potential shifts nor in corrosion. All of the more recent investigations of stray current induced corrosion on cathodically protected pipelines confirm that the electric charge will not be consumed for the corrosion reaction as long as the steel surface is passive.[5,23-28] Hence, anodic current discharge is not inevitably related to a corrosive dissolution of the metal following Faraday's law, i.e., an anodic current does not always result in corrosion. This is due to the fact that the anodic charge is consumed for the reaction Fe(II)/Fe(III) on the passive surface, rather than the reaction Fe(0)/Fe(II) in the case of time-variant stray current interference.

The criteria for stray current interference specified in EN 50162 are, however, based on the assumption of a time-constant anodic stray current load. Hence, it is required to discuss the effects of a time-constant anodic current on the corrosion processes. In the case of a time-constant anodic current, it is not possible to achieve an increase of the pH at the steel surface. In fact, a time-constant anodic current results in a decreasing pH value and thus in an acidification (caused by concentration polarization) at the steel surface leading to corrosion according to Figure 3(b). Moreover, the effect of a decreasing pH value is illustrated with the "time constant" arrow in Figure 4. The formation of an acidic electrolyte provokes corrosive conditions and passivation will be impossible. Under such circumstances, it is to be expected that 100% of the anodic current is consumed by the redox system Fe(0)/Fe(II), i.e., for the corrosion reaction. This underlines that EN 50162, which had been elaborated for time-variant interference from DC-operated railways or trams, is based on incorrect assumptions: the relevant increase of the pH value as a result of effective CP, which is crucial for the effectiveness of CP, the resulting passivation, the relevance of the redox system Fe(II)/Fe(III), and also the consequences of a CP current that is cathodic when averaged over a representative period of time, are ignored.

Based on the above discussed aspects, various influencing factors can be identified, which relevantly control the corrosion under time-variant stray current interference: anodic current will decrease the pH, while cathodic current will result in an increase of pH at the steel surface. It immediately follows that the average current over a full interference cycle (e.g., 24 h) represents a relevant parameter. This is due to the fact that the current efficiency for alkalinity formation is at least as good as the one for acidity formation in the case of steel. An average cathodic current is therefore bound to result in a pH increase over time irrespective of temporary anodic excursions. Hence, the polarity of the average electrical charge controls the direction of pH change at the steel surface. This effect of concentration polarization can best be illustrated based on an analogy: in the absence of anodic current discharge or in the case of cathodic interference a reservoir of alkalinity is accumulated at the steel surface. This reservoir will be consumed during anodic current discharge. Saving alkalinity provides, therefore, corrosion protection during the hard times under anodic current discharge. As long as more alkalinity is saved than consumed, an increased surface pH and hence corrosion protection is ensured even under severe time-variant anodic stray current interference. Indeed, experience confirms that there is no detrimental effect with respect to corrosion caused by loss of surface pH under such conditions of very short anodic polarization in the range of 10 ms (Figure 4). As a consequence, the process is run as an activation polarization controlled oxidation and reduction of Fe(II)/Fe(III), and the contribution of concentration polarization can be neglected as a result of the high frequency. However, based on the argumentation in EN 50162, this anodic current would have to result in relevant metal loss as a result of Faraday's law and an assumed oxidation of Fe(0)/Fe(II).

In contrast, a duration of the anodic interference of 30 s causes a relevant temporary change of the surface pH during the anodic excursion, although the time averaged current is cathodic (Figure 4). Such durations are typical for tram operation. A further increase of the duration of the anodic interference to 250 s, as is characteristic for DC train operation, can cause a major loss of surface pH resulting in temporary initiation of corrosion (250 s arrow in Figure 4). While the subsequent

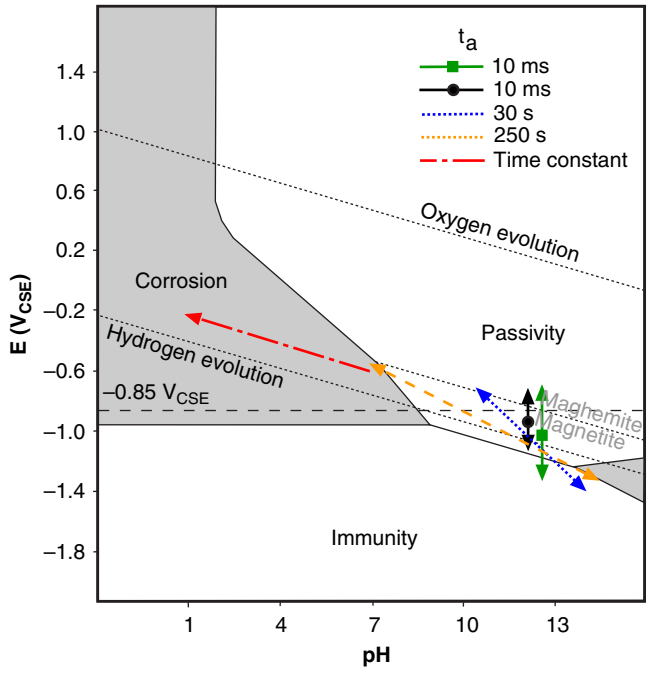

FIGURE 4. *Polarization of steel under stray current interference illustrated in the Pourbaix diagram[15] as a function of the duration of the anodic interference (t_a). The time-constant anodic interference results in concentration polarization and corrosion (e.g., in case of ineffective CP). A time-variant interference in the case of effective CP is illustrated with the various double arrows. The different duration of the anodic interference of 10 ms, 30 s, and 250 s results in different levels of concentration polarization at a given cathodic charge. The effects under AC interference are shown for J_{dc} > 1 A/m^2 (10 ms square) and J_{dc} < 1 A/m^2 (10 ms disk).*

cathodic interference will re-establish passivating conditions according to Figure 4, a non-negligible corrosion rate will be observed in this interference situation. According to the above discussion, the current efficiency based on the reaction Fe(0)/Fe(II) will be smaller than 100%, because only a fraction of the anodic charge is consumed for corrosion. This effect is indeed experimentally observed in the case of time-variant anodic interference.[29] Correspondingly, the decreasing frequency of interference increases the contribution of concentration polarization and associated surface pH changes.

The ratio of the anodic and cathodic charge is relevant with respect to concentration polarization and hence the pH at the steel surface. The assessment of the corrosion risk can, therefore, be performed based on Equation (1) with the anodic interference charge Q_a (total anodic surface in Figure 5[a]) and cathodic interference charge Q_c (total cathodic surface in Figure 5[a]) over the representative period of time.

$$Q \leq (|Q_c| - |Q_a|)/|Q_a| \quad (1)$$

The value on the right-hand side of Equation (1) describes the ratio of anodic and cathodic charge. For identical charges a value of zero is obtained. When the cathodic charge is double the anodic charge, it equals 1. Q describes the lower threshold with respect to the assessment of the stray current risk.

The Equation (1) emphasizes the relevance of the current density for the assessment of the anodic stray current corrosion risk. This is fully in line with the generally accepted behavior shown in Figure 2. However, a criterion based on current densities has significant limitations in the practical application, as current densities cannot be directly measured on the pipeline. Based on Ohm's law it is, however, possible to translate the current density consideration into a potential consideration under the following assumptions:

- The polarization resistances for anodic and cathodic reactions are small compared to the spread resistance of individual coating defects. This is indeed the case for both the hydrogen evolution as well as the redox system Fe(II)/Fe(III).
- The spread resistance does not relevantly change during the cathodic and anodic interference. This might not be the case during extended interference durations, but the cathodic interference will always result in lower spread resistance (and hence smaller potential change) compared to the anodic interference. This assumption is, therefore, conservative.

Indeed, the German technical rule DVGW GW 21[22] performs an assessment of the stray current corrosion risk on the basis of potential values. In the case of DC traction interference, a sufficient level of CP is present when Equation (2) is satisfied:

$$E_{on,avg} \leq E_{ref} - \Delta E_{a,avg} \quad (2)$$

The on-potential averaged over 24 h ($E_{on,avg}$) must accordingly be more negative than the reference potential (E_{ref}) minus the average anodic interference ($\Delta E_{a,avg}$). Similarly to the

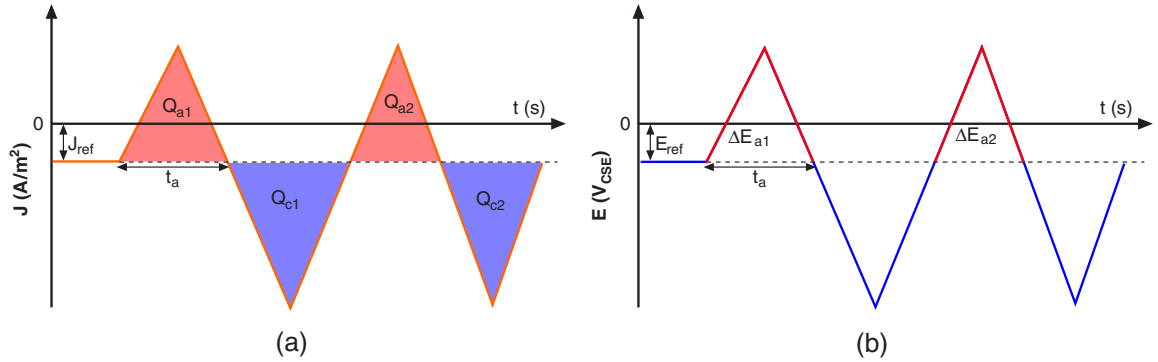

FIGURE 5. *Schematic evolution of stray current interference of a pipeline for current density in a coating defect or a coupon (a) and pipeline potential (b). The cathodic and anodic charges in (a) are obtain based on the surface integral of the respective current densities. The anodic interference $\Delta E_{a,avg}$ in (b) is the result of the average anodic shift of the potential relative to E_{ref}. The duration t_a corresponds to the longest anodic excursion.*

charge consideration in Equation (1), a stronger anodic interference can hence be compensated by larger cathodic charge, which is obtained at a more negative average on-potential. In Figure 5(b), the analogy between the current density (see Figure 5[a]) and the potential evolution is evident. E_{ref} corresponds to the minimal required on-potential in absence of DC interference for establishing effective CP. E_{ref} correspondingly ensures J_{ref}. $E_{on,avg}$ is the time average of all on-potential values recorded over a representative period of time. $\Delta E_{a,avg}$ corresponds to the average of all anodic potential values minus E_{ref}. Equation (2) was first published in 2009 and has today the status of a recognized state of the art in Germany. It is applicable for DC traction interference where typical maximum values of t_a of about 250 s are observed.

In the following the analogy between Equations (1) and (2) is further discussed. For the special case of $(|Q_c| - |Q_a|)/|Q_a| = 1$ of Equation (1) in combination with Equations (2) and (3) is obtained.

$$(|Q_c| - |Q_a|)/|Q_a| = (E_{ref} - E_{on,avg})/\Delta E_{a,avg} \quad (3)$$

The validity of Equation (3) has been mathematically demonstrated in Büchler, et al.[30] Because Equation (3) cannot be intuitively understood, the equivalence between Equations (1) and (2) will be further discussed in the following. For this consideration it is assumed that the anodic and cathodic interference in Figure 5(b) are identical. In this case it follows immediately that $E_{on,avg} = E_{ref}$. Equation (2) can hence only be satisfied, if $E_{on,avg}$ is shifted by $\Delta E_{a,avg}$ in the cathodic direction. As a consequence, Equation (2) requires that the cathodic interference must be at least the double of the anodic interference. This corresponds exactly to the requirement of Equation (1) with $(|Q_c|-|Q_a|)/|Q_a| = 1$, which demonstrates the validity of Equation (3).

A further aspect of the assessment of the corrosion risk caused by stray current interference is obtained when the minimum ratio Q of the anodic and cathodic charge required for effective corrosion protection is variable (and not set to 1). In this case Equations (4) and (5) are obtained:

$$Q = (|Q_c| - |Q_a|)/|Q_a| \quad (4)$$

$$Q = (E_{ref} - E_{on,avg})/\Delta E_{a,avg} \quad (5)$$

The DVGW GW 21[22] is only valid for interference caused by DC traction systems. The question raises whether the applicability of Equations (4) and (5) can be extended to lower frequency, as it is usually associated with tidal and telluric interference.

Based on the above discussion of high-frequency interference, it can be concluded for values of $t_a \rightarrow 0$ s that $Q \rightarrow 0$ with respect to corrosion protection against anodic charge transfer. With Q approaching zero the anodic and the cathodic interference required for corrosion protection become identical. This requirement is the direct consequence of a negligible duration of the anodic current discharge, which does not provide time for diffusion and migration of the hydroxide ions generated at the steel surface into the adjacent soil. Additionally, DVGW GW 21[22] requires a value of Q = 1 for DC traction interference, which typically has a maximum value of t_a = 250 s. Hence, it is possible to extrapolate from t_a = 0 s and t_a = 250 s to longer interference conditions. This results in Equation (6) as the minimum requirement with respect to protection against stray current induced corrosion:

$$Q = t_a \times 0.004 s^{-1} = (|Q_c| - |Q_a|)/|Q_a|) = (E_{ref} - E_{on,avg})/\Delta E_{a,avg} \quad (6)$$

It can be assumed (see Equation [2] from DVGW GW 21) that higher values of $(|Q_c|-|Q_a|)/|Q_a|$ than the minimum requirement of $Q = t_a \times 0.004\ s^{-1}$ will also ensure protection against stray current induced corrosion. Hence, an assessment criterion according to Equation (7) is obtained:

$$Q = t_a \times 0.004 s^{-1} < (|Q_c| - |Q_a|)/|Q_a|) = (E_{ref} - E_{on,avg})/\Delta E_{a,avg} \quad (7)$$

It is evident that the risk with respect to stray current induced corrosion can be assessed based on the concepts of DVGW GW 21[22] over the entire frequency domain. The validity of this approach is confirmed by the data in Figure 6. These measurements were performed in artificial soils as described in Büchler and Schöneich[3] and in hard water with the calcium containing electrolyte given in Büchler, et al.[31] A galvanostatic saw tooth shaped (according to Figure 5[a]) current density was applied to electrical resistance coupons (ER coupons) with a surface of 1 cm^2. The current variation (anodic peak/cathodic peak) was 2 A/m^2. Various values for J_{ref} and t_a were applied. The dotted line in Figure 6 corresponds to the requirement of $t_a \times 0.004\ s^{-1}$ that was derived from DVGW GW 21.[22]

The results in Figure 6 confirm the validity of the requirements of DVGW GW 21 with respect to t_a = 250 s and hence the correctness of the underlying investigations of Bette and Schulte.[29] Additionally, it is evident that the concept of DVGW GW 21 can be extrapolated to values of t_a of several hours. In no cases were unacceptable corrosion rates observed when Equation (7) was satisfied.

The crucial advantage of Equation (7) is the expansion of the application range of the DVGW GW 21 to the entire frequency domain of anodic stray current interference. This domain ranges from AC frequencies (t_a = 0.01 s) over DC traction interference (t_a = 250 s) and tidal interference (t_a = 22,000 s) to time-constant interference (t_a = infinite).

For small values of t_a in the range of 0.01 seconds, Q will approach zero according to Equation (2). As a consequence, the anodic interference may be almost equivalent to the cathodic interference. Based on Equation (7), $E_{on,avg}$ only has to be more negative than E_{ref} in order to prevent stray current induced corrosion as a result of anodic charge transfer. This is indeed confirmed by extensive field investigations in Germany.[32-34] Based on these data, no corrosion is expected even in the case of AC current densities as high as several hundred A/m^2 at appropriately negative average on-potentials (e.g., between −1.2 V_{CSE} and −1.0 V_{CSE}).

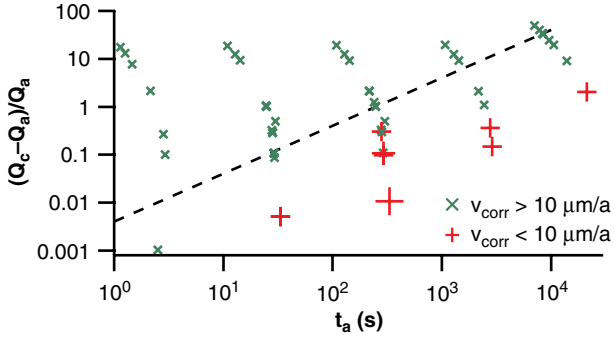

FIGURE 6. *Experimental determination of Q as a function of t_a in artificial soil and hard water. The dotted line represents the minimum requirement for protection against stray current corrosion, i.e., $(|Q_c|-|Q_a|)/|Q_a| = t_a \times 0.004\ s^{-1}$.*

In Annex D of EN 50162 a method for assessing the stray current corrosion risk caused by DC traction systems is presented. This method was developed in the Netherlands and was successfully used during the last 25 y. It is based on the limitation of the current discharge from a steel coupon to only 3.6 s during the hour with the highest stray current interference. Considering a typical cycle duration of several minutes during DC traction interference, the acceptable duration t_a of the anodic interference during an individual stray current interference period is less than 1 s. While the duration of anodic stray current discharge is strictly limited, the level of the anodic current discharge during this anodic interference is not restricted based on Annex D in EN 50162 and it could theoretically reach very high values. This significant limitation of t_a to values of less than 1 s generates at first glance the impression that this successfully used methodology is significantly more conservative than the one in Equation (7). However, the Annex D and Equation (7) are in fact in very good agreement, when the operation conditions of CP in the Netherlands during the last decades are considered. The effectiveness of CP was usually assessed based on an on-potential that was controlled in the range between −0.85 V_{CSE} and −1.2 V_{CSE}. Hence, $E_{on,avg}$ was very close (or even identical) to E_{ref}. Without strict limitation of $\Delta E_{a,avg}$, Equation (7) can only be satisfied at almost identical $E_{on,avg}$ and E_{ref}, if t_a is extremely small. Indeed, Annex D of EN 50162 does not limit $\Delta E_{a,avg}$ and t_a is extremely small (i.e., less than 1 s). There is wide consensus in Europe that these requirements in Annex D are very conservative. This conclusion is plausible, because most CP systems in Europe are operated at $E_{on,avg}$ more negative than −1.6 V_{CSE}. As a consequence, significantly higher values of t_a can be tolerated according to Equation (7). The example of AC interference as well as the very small values of t_a in Holland (reported in Annex D of EN 50162) are therefore fully in line with the presented methodology.

Equation (7) is also confirmed for very large values of t_a, as they are observed in the case of time-constant stray current interference. In this case, Q becomes infinite and Equation (7) can only be satisfied when the anodic charge (or $\Delta E_{a,avg}$) approaches zero. This is indeed only possible if Equation (8) is fulfilled:

$$E_{on} \leq E_{ref} - \Delta E_{a,max} \quad (8)$$

The on-potential must be shifted in the cathodic direction by the maximum anodic shift ($\Delta E_{a,max}$). This eliminates any anodic interference and Q_a becomes zero satisfying Equation (7). Indeed, this is a common procedure for mitigation of time-constant anodic stray current interference.

This consideration confirms the relevance of Equation (7). It is well established by practical application in the last 10 y in Germany and can be expanded to cover the entire frequency domain of anodic stray current interference ranging from AC interference to time-constant anodic DC interference. It allows for an assessment of the stray current corrosion risk as well as the identification and control of mitigation measures based on readily measurable potential data followed by an averaging process. The above procedure is introduced in ISO/DIS 21857.

THE EFFECT OF CATHODIC STRAY CURRENT INTERFERENCE

The above discussion of anodic stray current interference has highlighted the relevant processes taking place under anodic stray current discharge. It has been shown that these concepts can be expanded to explain all the effects taking place over the entire frequency domain including the AC interference condition that is included in the scope of ISO/DIS 21857. This raises the question with respect to the relevance of ISO 18086 that also covers criteria with respect to AC corrosion. This apparent conflict can readily be resolved when taking into account the relevant mechanism of AC corrosion: the above discussion with respect to anodic interference has clearly shown that AC corrosion as a result of anodic interference cannot occur as long as effective CP is established by applying an average on-potential more negative than E_{ref} (e.g., −1.0 V_{CSE}). This is well in line with most recent results of Moran and Lillard who reported no significant AC corrosion when a minimum level of CP was applied.[35] Based on this observation and the above discussion, AC corrosion as a result of anodic current discharge is effectively excluded by establishing effective CP, which is based on an increase of the pH value at the steel surface and the establishing of a protective passive film. Anodic current discharge is therefore irrelevant as long as the passivating conditions are maintained, which is indeed the case for the very short anodic excursions in the case of AC interference.

In contrast, ISO 18086 does not cover the corrosion aspects of anodic stray current interference, but those caused by excessive cathodic polarization. Indeed, the first leaks on cathodically protected pipelines occurred in over-polarization conditions at on-potentials more negative than −2 V_{CSE}.[36-37] Correspondingly, ISO 18086 limits the level of AC current density (J_{ac}) to less than 30 A/m^2 or the DC current density (J_{dc}) to less than 1 A/m^2. This implies that AC corrosion is an over-polarization problem, as limiting the level of cathodic current density is an effective measure that eliminates the AC corrosion risk. This can readily be explained when the process of AC corrosion is considered in detail according to: Büchler and Schöneich[3] and Büchler.[38] In Figure 4, this process can be followed by means of the double arrow (10 ms square). During the anodic half-cycle, the steel surface is oxidized resulting in activation polarization into the passivity domain as a result of the anodic current, leading to the formation of a passive film. This passive film effectively prevents the occurrence of any corrosion. During the cathodic half-wave, this passive film is electrochemically dissolved due to activation polarization into the immunity domain and thus converted into a porous layer of rust. This rust layer has a composition comparable to magnetite or the corresponding hydroxide and contains the above mentioned redox system Fe(II)/Fe(III) (see dashed line marked maghemite/magnetite in Figure 4). In the subsequent anodic cycle, a new passive film is formed under the porous, nonprotective rust layer. Moreover, the Fe(II) present in the rust layer will be oxidized to Fe(III). In the subsequent cathodic cycle, the oxidized rust layer will be reduced again (Fe[III] is reduced to Fe[II]) and in case of excessive cathodic charge, the activation polarization into the immunity domain will result in the cathodic dissolution of the passive film again. Hence, the rust layer will increase in thickness with every cycle, which is accompanied by a corresponding loss of steel. The amount of steel lost during each AC cycle is minimal and roughly corresponds to one atomic layer. However, running this process at a frequency of 50 Hz results in corrosion rates that are readily in the range of 1 mm/y. This discussion reveals some relevant aspects.

AC corrosion as a result of over-polarization is not caused by an activation-controlled anodic corrosion caused by oxidation of Fe(0) to a soluble Fe(II). Correspondingly, no soluble corrosion products are observed. The mechanism associated with

the formation and dissolution of the passive film were described by Schmuki, et al.,[39] as a solid-state conversion of the passive film to a rust layer. The corrosion products grow to significant sizes directly from the steel surface and are not formed by a dissolution and precipitation process as this is the case for anodic stray current interference associated with a pH decrease.

This intimate contact of the rust layer with the steel surface ensures the electron conductive connection between the two. As a consequence the redox system Fe(II)/Fe(III) remains electrically accessible. This readily explains the well-documented observation that J_{ac} may be in the range of several hundred A/m^2 without causing any metal loss. In contrast, the J_{dc} of more than 1 A/m^2 causes corrosion rates of more than 1 mm/y. Based on the above discussion this effect can readily be explained: the rust layer allows to pass virtually unlimited anodic and cathodic charge based on the redox system Fe(II)/Fe(III), preventing polarization into immunity and dissolution of the passive film. Various authors have reported the change of the oxidation state of this rust layer under the influence of an electrical current[39-41] on the passive steel surface. This prevents any AC corrosion from occurring. If, however, the average DC current density is large enough (>1 A/m^2) to result in a temporary activation polarization into the immunity domain, the passive film is cathodically dissolved and the corrosion mechanism is initiated. It has been demonstrated that AC corrosion can readily be controlled by means of limiting J_{dc} to values below 1 A/m^2.[38] This is illustrated in Figure 4 with the 10 ms disk double arrow. The decreased DC current density prevents polarization into immunity and cathodic dissolution of the protective passive film, thus preventing the occurrence of AC corrosion under over-polarization conditions and the resulting repeated formation and dissolution of the passive film.

The mechanism shown with the 10 ms disk double arrow in Figure 4 is not limited to 50 Hz. In fact, decreasing the frequency is expected to decrease the contribution of capacitive effects, which would make the corrosion process even more effective. Indeed, the 30 s and 250 s arrows in Figure 4 also cause repetitive activation polarization between immunity and passivity. As a consequence, the corrosion process described in ISO 18086 should not be limited to AC interference but would cover the entire frequency domain. Indeed, it has been demonstrated that the repeated formation and dissolution of the passive film occurs at cycle durations of 720 s.[42] However, decreasing the frequency from 50 Hz to a typical DC traction interference that has a cycle time of about 500 s (corresponding to a frequency of 2 mHz) will decrease the corrosion rate by a factor of 25,000. Consequently, the corrosion due to over-polarization will occur, but the rate is usually negligible at lower interference frequencies associated with typical traction interference. This explains the absence of any reported damages in this respect.

The complexity of these effects requires a more detailed discussion, in order to highlight the relevant processes taking place under AC interference conditions. The effect of AC interference on the actual IR-free potentials as a function of the current density (J) was recorded by Bette in artificial soils at a data acquisition rate of more than 1 kHz.[43] These results for two ER coupons are shown in Figure 7. The potential variation is a result of activation polarization, as the high-frequency limits relevant concentration changes under AC interference. Despite significantly increased J_{dc}, the $E_{IR\text{-}free}$ is temporarily anodic of the protection criterion of –0.85 V_{CSE} on both

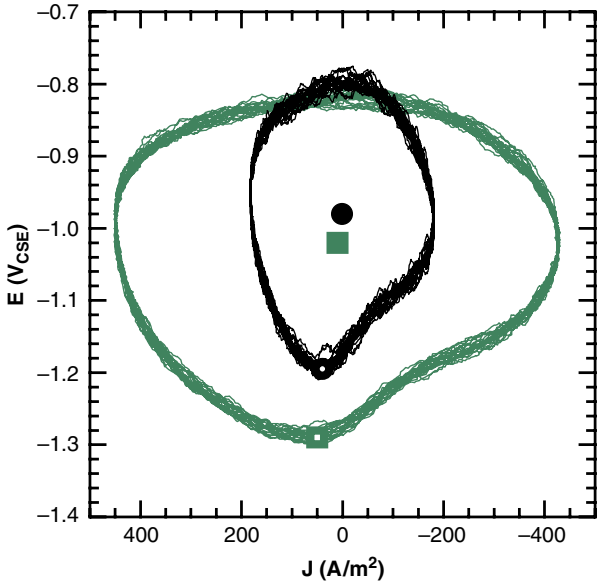

FIGURE 7. *IR-free potentials determined on ER coupons as a function of the current density (J) under AC interference of 16.7 Hz (cathodic currents with a positive sign). Disk symbols: no corrosion at J_{dc} 1 A/m^2, J_{ac} 128 A/m^2. Square symbols: corrosion at J_{dc} 11 A/m^2, J_{ac} 309 A/m^2 according to Bette.[43] The full symbols correspond to $E_{IR\text{-}free}$ and the empty symbols to the most negative cathodic excursion called E_H.*

coupons. Based on the concurrently recorded corrosion rate data, a metal loss is only observed when a temporary activation polarization cathodic of –1.2 V_{CSE} occurs. As discussed above, the activation polarization into immunity only occurs at J_{dc} larger than 1 A/m^2. Special attention must be paid to the time dependence of $E_{IR\text{-}free}$, which shows a variation of about 0.4 V as a function of the polarity of the current density (J). Based on the data in Figure 7, this time dependence can be assessed with a data acquisition rate of at least 1 kHz. Slower measuring rates of less than 10 Hz, as they are usually applied in CP for assessing the $E_{IR\text{-}free}$, do not show this time dependence due to the filter systems in the measuring instruments. Hence, the question regarding the physical significance of the various $E_{IR\text{-}free}$ in Figure 7 rises. In this context only the most relevant influencing factors and the corresponding conclusions will be addressed. A more detailed discussion of the involved processes is given in Büchler and Joos.[44]

Based on Figure 7 it is not possible to determine a single value for the $E_{IR\text{-}free}$. It is, however, possible to determine an average of all of the recorded values, which in a first approach corresponds to the classical slowly measured (about 100 ms after interrupting J_{dc}) $E_{IR\text{-}free}$. This value is illustrated with the full symbols in Figure 7. Additionally, in Figure 7 the most negative potential excursion limited by hydrogen evolution can also be determined, which according to the model concept controls the AC corrosion process. This parameter is in the following context described as E_H marked by means of the empty symbols in Figure 7. These data confirm the relevance of the J_{dc} and J_{ac} given in ISO 18086. They furthermore demonstrate that it is the excessive cathodic activation polarization rather than the anodic polarization which initiates the AC corrosion process by polarizing into immunity. For further illustration of this process, the surface pH was calculated based on the solid line in Figure 2. These pH values and the $E_{IR\text{-}free}$ data of Figure 7 are well in line

with the arrows for 10 ms shown in Figure 4. It is evident that the potential variation of Figure 7 is cathodically limited by hydrogen evolution and anodically by Fe(II)/Fe(III). This confirms the relevance of these redox systems with respect to the potential variation in the case of stray current interference. Clearly, there is no reason to expect a corrosion process as long as the potential remains within the passivity domain (data with disk symbols). Only excessive cathodic activation polarization causes the polarization into immunity at increased J_{dc} (data with square symbols). This initiates the process of repeated formation and dissolution of the passive film on steel and hence the AC corrosion process according to Büchler and Schöneich.[3] This effect shown in Figure 4 with the 10 ms double arrows is fully in line with the polarization into immunity and cathodic dissolution of the passive film[38] as a result of over-polarization at E_H more cathodic than −1.2 V_{CSE} at DC current densities of more than >1 A/m^2.

Based on this discussion and in particular based on the potential variation in Figure 7 it is possible to further elaborate the relevant processes taking place under AC interference. It follows from the above discussion that in absence of AC interference Equation (9) applies:

$$E_{IR\text{-}free} = E_H \tag{9}$$

In presence of AC interference Equation (10) applies with the contribution of the so-called Faradic rectification, ΔE_F.[45]

$$E_{IR\text{-}free} = E_H + \Delta E_F \tag{10}$$

This consideration represents a rough simplification of the processes taking place at the steel surface under exclusion of all time-dependent contributions. However, it provides a physical description for the empirically observed effects caused by the rectification of J_{ac}. The size and the polarity of ΔE_F are dependent on the ratio of the Tafel slopes of the anodic and cathodic activation-controlled reactions. It is characteristic for passive systems that ΔE_F has a positive sign. This effect was used for so-called "wet rectifiers" (or electrolytic rectifiers) in the past. Also, the DC decoupling devices based on nickel plates in KOH solution (the so-called polarization cells) are based on this effect. The key requirement for the electrodes used for wet rectifiers (and polarization cells) was their passivity (see e.g., Sebor and Simek[46]). This results in a large nonsymmetric current-potential behavior and a strong rectification.

The J_{dc}, which passes through a coating defect with a metallic surface of A, is the result of the difference between E_{on} and $E_{IR\text{-}free}$ as well as the spread resistance, R, according to Equation (10). For E_{on} more positive than −1.2 V_{CSE}, it was demonstrated that J_{dc} can approach zero.[38] Based on this concept it is possible to limit AC corrosion and satisfy the protection criterion of J_{dc} < 1 A/m^2 in ISO 18086 through the control of E_{on} even at very high levels of AC interference.

$$J_{dc} = \frac{E_{IR\text{-}free} - E_{on}}{R \cdot A} \tag{11}$$

The J_{ac} passing through the metal surface causes a shift of the $E_{IR\text{-}free}$ in positive direction according to Equation (10) and as illustrated with the full symbols in Figure 7 with respect to the empty symbols. For the determination of J_{dc} the $E_{IR\text{-}free}$ (average $E_{IR\text{-}free}$) is relevant, which is a result of E_H and ΔE_F. The evaluation of the literature data[3] with respect to J_{ac} and the resulting anodic shift of $E_{IR\text{-}free}$ under assumption of a linear behavior allows describing ΔE_F with a factor f according to Equation (12).[47-48]

$$\Delta E_F = f \cdot \frac{U_{ac}}{R \cdot A} \tag{12}$$

$$U_{ac} = R \cdot A \cdot (J_{dc} \cdot R \cdot A - E_H + E_{on})/f \tag{13}$$

The combination of Equations (11) and (12) results in Equation (13), which is a description of the E_{on} and the allowable U_{ac} as a function of the critical J_{dc} in the case of effective CP.

The further consideration of the thermodynamic[15] and kinetic[39,42] parameters with a mathematical description of the decrease of the spread resistance caused by the increase of the pH value at the steel surface as a result of J_{dc} and the resulting spread of alkalinity, as shown in Figure 3(a), allows for a more detailed description of the corrosion process under AC interference on the basis of Equation (13).[47-48] This detailed model concept allows for explaining the relevant discrepancy between the actual damages on pipelines and the high corrosion rate on coupons as described in Büchler.[49]

Based on Equation (13), the acceptable U_{ac} reaches a value close to zero for decreasing defect sizes. In contrast, an increase of the metallic surface A in the coating defect will increase the acceptable U_{ac}. This has a relevant implication, as any corrosion process will cause an increase of the metallic surface, as demonstrated in Büchler and Joos.[47-48] These considerations and the subsequent validation of the model have revealed that any AC corrosion process will reach negligible values once a certain corrosion depth has been reached. This is the result of the increase of the steel surface caused by the corrosion process and a direct consequence of the geometrical morphology of the corrosion site and Equation (13). If the soil resistivity (ρ), the average E_{on} and U_{ac}, the original coating defect size, and the allowable corrosion depth are known, an assessment of the acceptable interference conditions is possible. The key conclusions for AC corrosion are therefore as follows:

- At small coating defects AC corrosion cannot be prevented.
- AC corrosion will reach negligible rates at a certain depth.
- This depth is higher on large coating defects than on small coating defects.

These qualitative conclusions are in good agreement with the empirical observation of the last decades. Leaks due to AC interference were primarily observed on pipelines with small pipe wall thickness. Moreover, very high corrosion rates were found on thin coupons while only corrosion depths in the range of 1 mm to 2 mm were found on the associated pipelines.

Based on laboratory and field investigation, a numerical description of all influencing parameters was developed. In particular, the effect of pH increase at the steel surface and the migration of alkalinity into the surrounding soil (as shown in Figure 3[a]) was numerically described. The individual parameters were first calibrated in laboratory investigations and then validated in field tests.[47-48] The applicability of the model was thus demonstrated. Moreover, the expected influence of the metallic surface as a function of corrosion depth on the corrosion rate was confirmed. This validated model is in line with the empirical experience collected in the past 30 y. It allows, therefore, predicting the critical conditions and optimizing mitigation measures in the practical operation of pipelines. The resulting numerical model and the associated parameters were

introduced in 2018 into the technical rule DVGW GW 28 B1[50] that represents the recognized state of the art in Germany.

This model for AC corrosion can explain the discrepancy between the high corrosion rates observed on coupons and the very limited amount of damage on pipelines. The increase of the steel surface due to the corrosion process results with increasing corrosion depth in decreasing current densities. When they reach the threshold current densities stated in ISO 18086, the AC corrosion process is expected to reach negligible rates. Based on the important relevance of the corroding steel surface and hence the corrosion depth, the AC corrosion rate is strongly time dependent and of limited relevance. The very high corrosion rates in the early stages of AC corrosion decrease rapidly with progressing depth. Hence, it is impossible to extrapolate a corrosion rate determined over a limited exposure time to the operation time of the pipeline.

All of the available data demonstrate that the assessment of the acceptable interference level can only be based on an acceptable corrosion depth. The discussion of the critical coating defect surface[47-48] demonstrates that the assumption of a critical coating defect surface of 1 cm^2 already implies an acceptable corrosion depth in the range of 1 mm to 2 mm. The meeting of the requirements of ISO 18086 on coupons with 1 cm^2 defect surface cannot exclude higher current densities on smaller coating defects and hence corrosion. As predicted by the model calculation, these small coating defects never lead to perforation of pipelines. It is expected that they corrode rapidly in the early stages, but then the corrosion rate reaches negligible values within 1 mm to 2 mm depth. These considerations clearly show that the present standard has an implicitly accepted maximum corrosion depth, which confirms that the occurrence of AC corrosion in the range of a few millimeters cannot be excluded on any pipeline even when all applicable standards are applied.

The validation of the model allows for the assessment of the AC corrosion risk on pipelines caused by cathodic interference. The numerical description of the relevant influencing factors offers the possibility to correctly address them and optimize mitigation measures. Examples of this consideration for a maximum corrosion depth of 5 mm are shown in Figure 8.

Clearly, an important dependence of the admissible U_{ac} on ρ and E_{on} is found, demonstrating that it is impossible to define generally valid interference levels for U_{ac}. The requirements in Figure 8 allow for determining critical sections of the pipeline system as well as the development of mitigation strategies. Experience shows that, depending on the various factors, the highest corrosion risk is not necessarily associated with the highest U_{ac} induced on the pipeline, but rather low soil resistivity in combination with negative on-potentials.

With this approach shown in Figure 8 it is possible to demonstrate relevant differences between fusion bonded epoxy (FBE) coatings with thickness in the range of 0.5 mm and three-layer polyethylene coatings (PE) with thickness in the range of 2 mm. In the case of FBE, the corrosion products fracture the coating and the lateral extension of the corrosion process underneath the FBE coating is very limited. This characteristic behavior of FBE is usually described as "fail safe" as the access of CP current is ensured by the fracturing of the coating. In the case of AC corrosion, however, the defect diameter is increasing with the diameter of the corrosion site. This has relevant implications with respect to the damage mechanism according to the described model. Small coating defects result in high current densities and high corrosion rates. Instead of a fast decrease of the corrosion process to negligible values (as expected for PE), the coating defect diameter grows with increasing corrosion depth and allows for further extension of the corrosion process and the reaching of larger depths. This is expected to result in faster perforation of the pipeline in the case of FBE compared to PE coating, as the corrosion process is always running at the most critical condition, as described in Büchler and Joos.[47-48]

In contrast, the PE coating is mechanically more robust. The experience shows that it will be lifted off the steel surface through the mechanical pressure of the corrosion products, while maintaining the original coating defect diameter. The shielding of the activation-controlled AC corrosion process is, therefore, an advantage of PE coatings. Based on these considerations different parameters are required for addressing the AC corrosion risk on PE- and FBE-coated pipelines. This is readily possible with the two different parameter sets

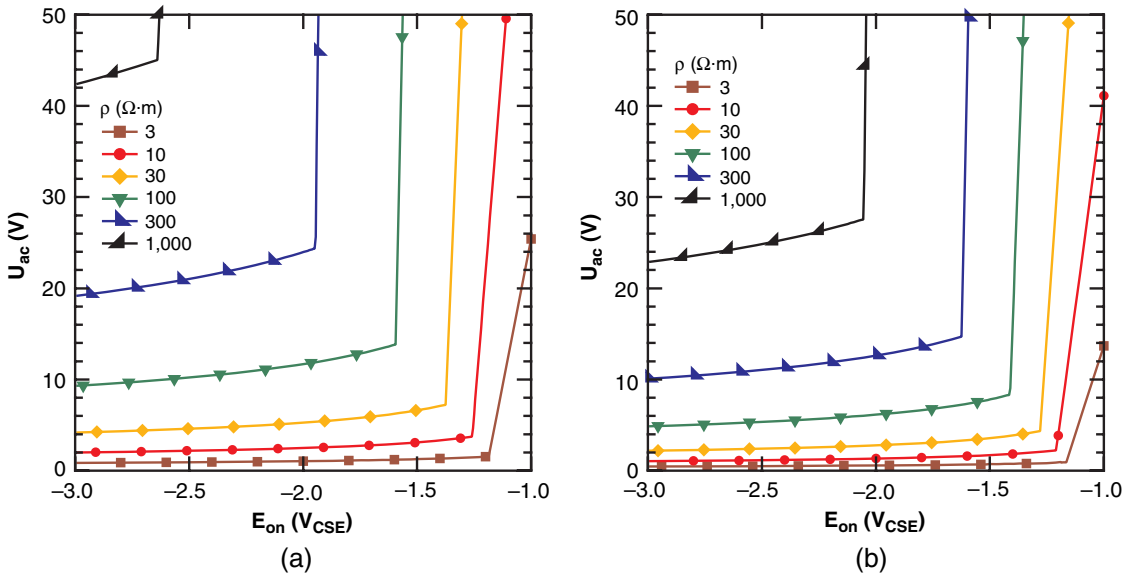

FIGURE 8. *Admissible average U_{ac} as a function of the average E_{on} for various soil resistivities ρ and an acceptable I_{max} of 5 mm calculated with the parameters in Büchler and Joos [47-48] for: (a) PE and (b) FBE coatings.*

proposed in Büchler and Joos[47-48] and the resulting thresholds shown in Figure 8.

This concept has formed the basis for the DVGW GW 28-B1.[50] No leaks have been reported in central Europe for PE-coated pipelines with wall thicknesses of more than 5 mm when the 24-h average values of U_{ac} and E_{on} given in Figure 8(a) for the different values of the soil resistivity ρ are not exceeded.

This concept allows the assessment of the AC corrosion risk based on readily available potential values and significantly facilitates the decision with respect to mitigation measures. Based on this approach, the critical sections on the pipeline are readily identified. The additional installation of coupons in these specific areas allows for demonstrating the correctness of the numerical analysis and the determination of the current densities required by ISO 18086. In the evaluation of these data, the relevance of processes described in Equation (13) and in Büchler and Joos[47-48] still need to be taken into account.

ASSESSING EFFECTIVENESS OF CATHODIC PROTECTION

Based on the presented model concepts on the mechanism of CP in combination with the effects taking place during anodic as well as cathodic stray current interference, a comprehensive description of all aspects of the associated corrosion processes has been determined. For the first time a unique procedure for addressing all influencing parameters in a single approach has been developed. Independent of the level and frequency of interference, the type of CP system, the type of coating, the presence of bonding of the pipeline, and the possibility to determine instant off-potentials, a straightforward assessment of the effectiveness of CP is now possible.

This approach is not limited to addressing the effectiveness of CP but takes into account also the conflicting requirements for mitigating DC interference and AC interference: DC interference with the risk of corrosion due to anodic polarization has to be addressed by shifting the on-potential more negative and AC interference with the risk of excessive cathodic polarization has to be mitigated by shifting the on-potential more positive. Based on this new approach, a straightforward analysis of all corrosion aspects and an optimized setting of the CP operation conditions are readily possible. Additionally, the identification of possible mitigation measures even in combined and complex interference situations can be performed. This new approach that is presently implemented in Switzerland will be shortly discussed in the following based on a hypothetical example. A PE-coated pipeline with a wall thickness of 5 mm in soil with a resistivity between 30 Ω·m and 100 Ω·m is assumed. The examples discussed in the following are based on a coating defect size on the PE-coated pipelines of 1 cm^2. Furthermore, a conservative value for J_{ref} of 0.1 A/m^2 is assumed that will ensure IR-free potentials well more negative than −1 V_{CSE} according to Figure 2. This approach requires three steps:

1. First E_{ref} needs to be determined. This value corresponds to the on-potential that is required to ensure J_{ref} and hence effective CP on all coating defects. Typical values for E_{ref} are between −1.0 V_{CSE} and −1.6 V_{CSE}. The assessment of E_{ref} can for example be based on $E_{IR\text{-}free}$ values in absence of DC interference on the pipeline, $E_{IR\text{-}free}$ values determined on coupons, or current density considerations taking into account Figure 2. In the given example, an E_{ref} of −1.05 V_{CSE} is determined as shown in Figure 9. In absence of stray current interference effective CP is ensured when the E_{on} is more negative than the E_{ref} line shown in Figure 9.
2. Second, the average anodic interference relative to E_{ref} is recorded over a representative period of time. For DC traction interference this is typically 24 h. In the present example, $\Delta E_{a,avg}$ was found to be about 0.4 V. The largest anodic interference period t_a is determined to be 250 s. According to Equation (7), a required $E_{on,avg}$ of about −1.45 V_{CSE} is calculated. This corresponds to the $E_{on,avg}$ line in Figure 9. Effective CP under anodic stray current interference is ensured when the E_{on} averaged over 24 h is more negative than the $E_{on,avg}$ line shown in Figure 9.
3. Third, the applicable interference line of Figure 8(a) for a PE-coated pipeline for the smallest soil resistivity is selected. In the present example, the soil resistivity ranges from 30 Ω·m to 100 Ω·m. Correspondingly, the line for 30 Ω·m is selected. These threshold values for the acceptable average U_{ac} are plotted in Figure 9 as U_{ac}. Effective corrosion protection is ensured when the 24 h average U_{ac} is below the U_{ac} line and the 24 h average E_{on} is more negative than the $E_{on,avg}$ line.

With this approach a straightforward assessment of effective corrosion protection is possible based on the present model concept of the mechanisms involved in CP. The example shown in Figure 9 emphasizes the conflicting requirements with respect to mitigating anodic stray current interference and AC interference. The mitigation of DC interference requires the shifting of the $E_{on,avg}$ to −1.45 V_{CSE}. It follows from Figure 9 that effective corrosion protection in this combined AC and DC interference situation can only be managed by lowering the average U_{ac} to values in the range of 5 V. In contrast, in absence of DC interference the risk of AC corrosion could effectively have been eliminated by applying a 24-h average on-potential in the range of −1.2 V_{CSE}. In this case, even significantly

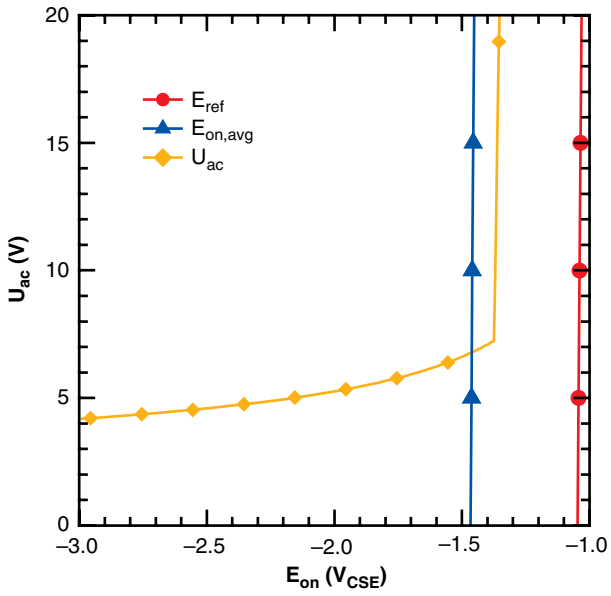

FIGURE 9. *Admissible average U_{ac} and average E_{on} for ensuring effective CP in case of combined DC and AC stray current interference: E_{ref} required to ensure effective CP with J_{ref} of 0.1 A/m^2 in absence of any interference; $E_{on,avg}$ for effective corrosion protection in case of anodic DC interference; and U_{ac} for protection against AC corrosion.*

increased levels of U_{ac} can be tolerated and mitigation of AC corrosion is possible based on a simple adjustment of the rectifiers rather than the installation of expensive earthing installations.

This discussion based on the concepts stated in the German documents DVGW GW 21[22] and DVGW GW 28 B1[50] highlights the new concepts that will allow for the assessment of effectiveness of CP on all types of pipelines, independent of their interference conditions. The identification of critical pipeline sections is possible based on readily accessible potential data, independent on the interference condition. Nevertheless, the use of a J_{ref} of 0.1 A/m^2 may not be realistic in all cases, as it will inadvertently lead to over-polarization conditions and associated issues with disbonding of coatings in heterogeneous soil conditions. This emphasizes the need for a more profound discussion of current density requirements and the influencing soil parameters. Based on Figure 2, even current densities as low as 1 mA/m^2 are expected to result in IR-free potentials of –0.85 V_{CSE} and increased pH at the steel surface. These aspects are presented and discussed in the literature.[51] Taking into account these influencing parameters, as well as the usually relevant variation of U_{ac} as well as $E_{on,avg}$ along the pipeline, will provide a more profound analysis of the level of corrosion protection, the assessment of critical areas for installation of coupons, and the identification of measures to ensure an optimum level of corrosion protection within conflicting normative requirements.

CONCLUSIONS

The presented discussion illustrates that the new understanding of the mechanisms involved in cathodic protection provides a comprehensive model that describes all influencing parameters. This model has some key consequences on a number of aspects that have not been appropriately addressed in the past:

➢ Cathodic protection is achieved by applying a cathodic current to a steel structure. While there is some contribution of an activation polarization at the very moment the current is applied, the relevant polarization that provides corrosion protection is a result of the concentration change at the steel surface. This change in concentration with respect to oxygen and hydroxide requires time to build up.

➢ Due to the time constants involved in concentration polarization, the corrosion protection is not lost when CP is interrupted or when anodic current discharge occurs. The slow diffusion processes associated with the loss of concentration polarization explain the relevance of 24-h average values and the irrelevance of anodic interference during time-variant stray current interference.

➢ Anodic stray current interference is irrelevant with respect to the integrity of pipelines as long as the concentration polarization (i.e., the increased pH at the steel surface) is maintained. Longer anodic interference can hence be compensated by means of an increased level of CP.

➢ At very low levels of CP (e.g., at on-potentials of –0.9 V_{CSE}), no anodic current discharge can be tolerated based on the presented concept due to the absence of sufficient concentration polarization.

➢ The new approach with respect to the assessment of effective CP under anodic stray current interference covers the entire frequency range of stray currents including AC interference, DC traction interference, tidal interference, telluric interference, and even time-constant anodic interference.

➢ While anodic AC interference has no relevance with respect to the integrity of pipelines in case of effective CP, high corrosion rates occur due to AC voltages in the case of over-polarization. Hence, AC corrosion is a problem associated with over-polarization caused by excessive CP or by cathodic interference.

➢ The effectiveness of CP can be assessed even in case of combined AC and DC interference. Based on the presented concepts the planning of mitigation measures and the assessment of their effectiveness are readily possible. Areas with high corrosion risk and possibly unacceptable conditions are identified. Based on this risk analysis, the locations for the installation of coupons or probes can be identified. Having coupons installed in the highest risk areas significantly increases the relevance of their readings.

➢ The presented concepts have the status of a recognized state of the art in Germany based on the technical rules DVGW GW 21[22] and DVGW GW 28 B1.[50]

The various aspects presented in this paper provide a complete description of cathodic protection and the relevant influencing parameters. Based on these concepts a new approach with respect to the assessment of the effectiveness of CP is possible. The effectiveness is determined based on the readily accessible average values of E_{on} and U_{ac}. This concept is applicable to all pipelines independent of the coating system, the interference conditions, the possibility to interrupt all CP current sources, the presence of galvanic anodes, and drainage bonds. Because all relevant influencing parameters are considered, an objective assessment of corrosion protection is possible. This approach allows for identifying areas with increased risk and the evaluation of mitigation measures. In areas with conflicting requirements, it may not be possible to find ideal solutions with respect to corrosion protection. Based on these concepts it will, however, be possible to operate the CP under optimized conditions while minimizing the corrosion risks caused by conflicting requirements. Considering the relevant associated costs of mitigation, the use of objective, technically correct, and justifiable assessment criteria is of highest importance.

References

1. L.I. Freiman, I.V. Strizhevskii, M.Y. Yunovich, *Prot. Met.* 24 (1988): p. 104.
2. F. Kajiyama, K. Okamura, *Corrosion* 55, 1 (1999): p. 74-80.
3. M. Büchler, H.-G. Schöneich, *Corrosion* 65 (2009): p. 578.
4. J.M. Leeds, *Pipe Line Industry* 4 (1992): p. 39.
5. N.G. Thompson, T.J. Barlo, "Fundamental Process of Cathodically Protecting Steel Pipelines," International Gas Research Conference (Rockville, MD: Government Institute, 1983).
6. U. Angst, M. Büchler, B. Martin, H.-G. Schöneich, G. Haynes, S. Leeds, F. Kajiyama, *Mater. Corros.* 67, 11 (2016): p. 1135-1142.
7. U.M. Angst, *Corrosion* 75, 12 (2019): p. 1420-1433.
8. M. Büchler, *MP* 54, 1 (2015): p. 44-48.
9. M. Büchler, "Cathodic Protection Criteria: The Mechanism of Cathodic Protection and Its Implications on the Assessment of Effectiveness of CP," NACE East Asia & Pacific Area Conference (Houston, TX: NACE International, 2019).
10. M. Büchler, "On the Mechanism of Cathodic Protection and Its Implications on Criteria Including AC and DC Interference Conditions," Advances in Corrosion Science and Corrosion Engineering (Melbourne, Australia: Australasian Corrosion Association, 2019).
11. R.J. Kuhn, *Ind. Eng. Chem.* 22, 4 (1930): p. 335-341.
12. W.v. Baeckmann, W. Schwenk, W. Prinz, *Handbuch des kathodischen Korrosionsschutzes Theorie und Praxis der elektrochemischen Schutzverfahren* (Weinheim, Germany: VCH Verlagsgesellschaft, 1989).

13. T.J. Barlo, "Field Testing the Criteria for Cathodic Protection of Buried Pipelines," PRCI, 1994.
14. W.v. Baeckmann, *Taschenbuch für den kathodischen Korrosionsschutz*, 6th ed. (Essen, Germany: Vulkan Verlag, 1996).
15. M. Pourbaix, *Atlas of Electrochemical Equilibria in Aqueous Solutions* (Houston, TX: NACE, 1974).
16. A.W. Peabody, *Control of Pipeline Corrosion*, ed. R.L. Bianchetti, 2nd ed. (Houston, TX: NACE, 2001).
17. A. Junker, L.V. Nielsen, "AC Corrosion and the Pourbaix Diagram," CEOCOR International Congress 2018 (Brussels, Belgium: CEOCOR, 2018).
18. A. Brenna, M.V. Diamanti, L. Lazzari, M. Ormellese, "A Proposal of AC Corrosion Mechanism in Cathodic Protection," Tech. Proc. of NSTI Nanotechnology Conference and Expo (Danville, CA: NSTI, 2011).
19. S. Msallamova, P. Novak, D.M. Kouril, presented at Metal 2015, Brno, Czech Republic, 2015, available at http://www.metal2015.com/files/proceedings/21/papers/3679.pdf.
20. D. Funk, H. Hildebrand, I.W. Prinz, W. Schwenk, *Werkst. Korros.* 38, 12 (1987): p. 719-724.
21. D. Joos, M. Büchler, "An Objective Discussion of Cathodic Protection Criteria Based on Literature Data," CEOCOR International Congress 2017 (Brussels, Belgium: CEOCOR, 2017).
22. DVGW GW 21 Arbeitsblatt, "Beeinflussung von unterirdischen metallischen Anlagen durch Streuströme von Gleichstromanlagen; textgleich mit der AfK-Empfehlung Nr. 2" (Bonn, Germany: DVGW, 2014).
23. L.I. Freiman, E.G. Kuznetsova, *Protect. Met.* 37 (2001): p. 484-490.
24. M. Ormellese, A. Brenna, L. Lazzari, F. Brugnetti, "Effects of Anodic Interference on Carbon Steel Under Cathodic Protection Condition," EUROCORR 2014 (Frankfurt, Germany: Dechema e.V., 2014).
25. L. Sanders, E. Fleury, S. Fontaine, V. Vasseur, "DC Stray Currents: Evaluation of the Relevance of the Risk Assessment Criterion Proposed by the European Standard EN 50162 - Part 2," EUROCORR 2017 (Frankfurt, Germany: Dechema e.V., 2017).
26. T. Nagai, H. Yamanaka, A. Nishikawa, H. Nonaka, "Influence of Anodic Current on Corrosion Protection Conditions of Buried Steel Pipeline Under Cathodic Protection," CORROSION 2017 (Houston, TX: NACE, 2017).
27. T. Nagai, H. Yamanaka, A. Nishikawa, H. Nonaka, "Influence of Instantaneous Potential Fluctuations on Corrosion Protection Conditions of Buried Steel Pipelines Under Cathodic Protection," NACE East Asia & Pacific Area Conference (Houston, TX: NACE International, 2019).
28. M. Attarchi, A. Brenna, M. Ormellese, "Cathodic Protection and DC Non-Stationary Anodic Interference: Criteria and Electrochemical Processes," EUROCORR 2019 (Frankfurt, Germany: Dechema e.V., 2019).
29. U. Bette, T. Schulte, *3R Int.* 44 (2005): p. 392.
30. M. Büchler, D. Joos, H.-G. Schöneich, "Assessing the Risk of Stray Current Induced Corrosion: Protection Criteria Developed Based on the Present Understanding of the Involved Processes," CEOCOR International Congress 2018 (Brussels, Belgium: CEOCOR, 2019).
31. M. Büchler, C.-H. Voûte, H.-G. Schöneich, "The Effect of Variation of A.C. Interference Over Time on the Corrosion of Cathodically Protected Pipelines," CEOCOR International Congress (Brussels, Belgium: CEOCOR, 2009).
32. M. Büchler, D. Joos, C.-H. Voûte, *DVGW-Energie Wasser Praxis* Juli/August 2010 (2010): p. 8.
33. M. Büchler, U. Angst, *DVGW-Energie Wasser Praxis* 6/7 (2016): p. 12.
34. M. Büchler, D. Joos, *DVGW-Energie Wasser Praxis* November 2013 (2013): p. 13.
35. A. Moran, R.S. Lillard, *Corrosion* 75, 2 (2019): p. 144-146.
36. B. Meier, *GWA* 69 (1989): p. 193.
37. G. Heim, G. Peez, *3R Int.* 27, 5 (1988): p. 345.
38. M. Büchler, *Mater. Corros.* 63, 12 (2012): p. 1181.
39. P. Schmuki, M. Büchler, S. Virtanen, H.S. Isaacs, M.P. Ryan, H. Böhni, *J. Electrochem. Soc.* 146, 6 (1999): p. 2097-2102.
40. D.D. Macdonald, B. Roberts, *Electrochim. Acta* 23, 8 (1978): p. 781.
41. R.S.S. Guzmán, J.R. Vilche, A.J. Arvia, *Electrochim. Acta* 24, 4 (1978): p. 395.
42. M. Büchler, P. Schmuki, H. Böhni, *J. Electrochem. Soc.* 144, 7 (1997): p. 2307-2312.
43. U. Bette, *3R Int.* 44 (2013).
44. M. Büchler, D. Joos, *3R* 6/2016 (2016): p. 52.
45. I. Ibrahim, M. Meyer, B. Tribollet, H. Takenouti, S. Joiret, S. Fontaine, H.-G. Schöneich, "On the Mechanism of AC Assisted Corrosion of Buried Pipelines and Its CP Mitigation," IPC 2008, paper no. 64380 (New York, NY: ASME, 2008), p. 601-625.
46. J. Sebor, L. Simek, *Z. Elektrochem.* 13 (1908): p. 113.
47. M. Büchler, D. Joos, "AC-Corrosion on Cathodically Protected Pipelines: A Discussion of the Involved Processes and Their Consequences on Mitigation Measures," EUROCORR 2016 (Frankfurt, Germany: Dechema e.V., 2016).
48. M. Büchler, D. Joos, *Ochrona przed Korozja* 61, 8/18 (2018): p. 204.
49. M. Büchler, "Determining the A.C. Corrosion Risk of Pipelines Based on Coupon Measurements," CEOCOR International Congress 2013 (Brussels, Belgium: CEOCOR, 2013).
50. DVGW GW 28-B1 (A), "Beurteilung der Korrosionsgefährdung durch Wechselstrom bei kathodisch geschützten Stahlrohrleitungen und Schutzmassnahmen: Beiblatt 1: Modifizierte Kriterien für Wechselspannung und Einschaltpotential" (Bonn, Germany: DVGW, 2018).
51. "Cathodic Protection Effectiveness: A Review of Protection Criteria, Threshold Values, and Evaluation of Alternative Methods," EPRI, reference 3002010674, 2017.